

Self-Organized Growth of Nanosized Vertical Magnetic Co Pillars on Au(111)

O. Fruchart,* M. Klaua, J. Barthel, and J. Kirschner

Max-Planck-Institut für Mikrostrukturphysik, Weinberg 2, D-06120 Halle, Germany

(Received 7 June 1999)

Starting from the conventional self-organized arrays of flat Co dots on Au(111), we extended the growth vertically to fabricate Co pillars. The principle is to deposit sequentially a fraction x of an atomic layer (AL) of Co and $1 - x$ AL of Au. At each step, the deposited Co atoms aggregate on top of the previous dots, increasing their height by 1 AL. Pillars with a 2:1 vertical aspect ratio were achieved. Because of the large number of atoms per pillar, the superparamagnetic blocking temperature is 300 K in the pillars, whereas it is only 20 K in conventional flat dots with the same lateral density.

PACS numbers: 68.65.+g, 75.70.-i, 81.05.Zx, 81.15.-z

The fabrication and study of magnetic ultrathin films has been largely stimulated by new phenomena arising from the reduction of dimensionality, from 3D in the bulk to 2D in ultrathin films. Lithography and etching techniques are now widely used to reduce lateral dimensions as well, to study well-defined 1D or 0D structures. Self-assembly and self-organization are a low-cost, alternative way to fabricate materials structured down to a few nanometers [1,2]. The terms “assembly” and “organization” are sometimes used interchangeably in the literature. In this Letter, we will use “self-assembly” when the deposited adatoms cluster into randomly distributed dots (0D), and “self-organization” when the dots form a regular array, at least on the medium range.

However, in the case of magnetism, such materials can not be used in devices. Indeed, self-organized dots with a high-density packing are rather flat and of small lateral extension, so that their volume V is extremely small. This implies that their anisotropy barrier KV is small (K is the anisotropy constant per unit volume), so that they are superparamagnetic [3] down to very low temperatures. Besides, the small value of V cannot be compensated by a high value of K , because anisotropy fields of the order of several tens of teslas would be required to get a blocking temperature $T_B > 300$ K. Therefore, the use of self-assembled and self-organized dots at 300 K seems at first sight not compatible with a high-density packing. In fact, the only possible solution is to increase V by using vertical pillars instead of flat dots. However, no vertical pillars could ever be fabricated by self-assembly and self-organization so far.

Nevertheless, fabricating vertical self-assembled structures is not a completely new idea. Some kind of vertical structure has already been reported by Xie *et al.* [4]. These authors fabricated multilayers of self-assembled quantum dots of InAs on GaAs. They observed that dots from successive layers show a tendency to stack vertically, due to lateral modulation of strain in the GaAs spacer layers. The in-plane self-assembly therefore evolves progressively into 3D self-organization (Fig. 1a) [4,5].

The growth process reported in this Letter is derived from this example. We show that, by reducing the

spacer layer thickness, it is possible to bring the dots from successive layers in direct vertical contact (Fig. 1b). Vertically stacked magnetic dots are then magnetically coupled, and behave as a single entity (a magnetic pillar). We demonstrate the feasibility of the process with Co on Au(111), starting from the well-known self-organized arrays of nanosized Co dots on Au(111) [1]. We will see below that self-organization is interesting for demonstration purposes, because the vertical replication of the regular array, observed straightforwardly on STM pictures, allows one to deduce that dots from successive layers are stacked. The reader should, however, keep in mind that the process would work as well starting from self-assembled dots (i.e., not organized). Besides, we will argue that the process is not specific to Co and Au, and that it should occur for other pairs of materials.

The experiments were performed under ultrahigh vacuum (base pressure below 5×10^{-11} mbar). Co and Au were evaporated from a rod and a crucible with deposition rates of 0.02 and 0.45 AL min^{-1} , respectively. STM images were recorded 30 min after deposition, to allow the sample to cool down. Polar and longitudinal magneto-optical Kerr effect loops were performed *in situ* in the field range $\pm 0.8T$.

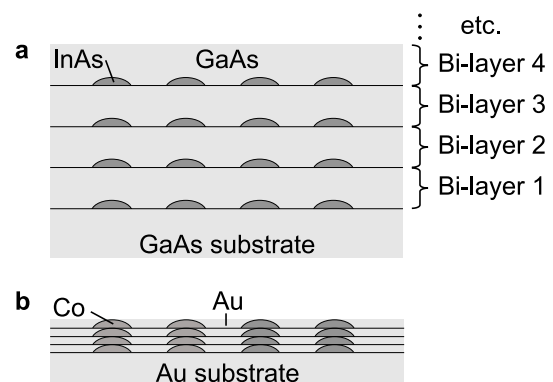
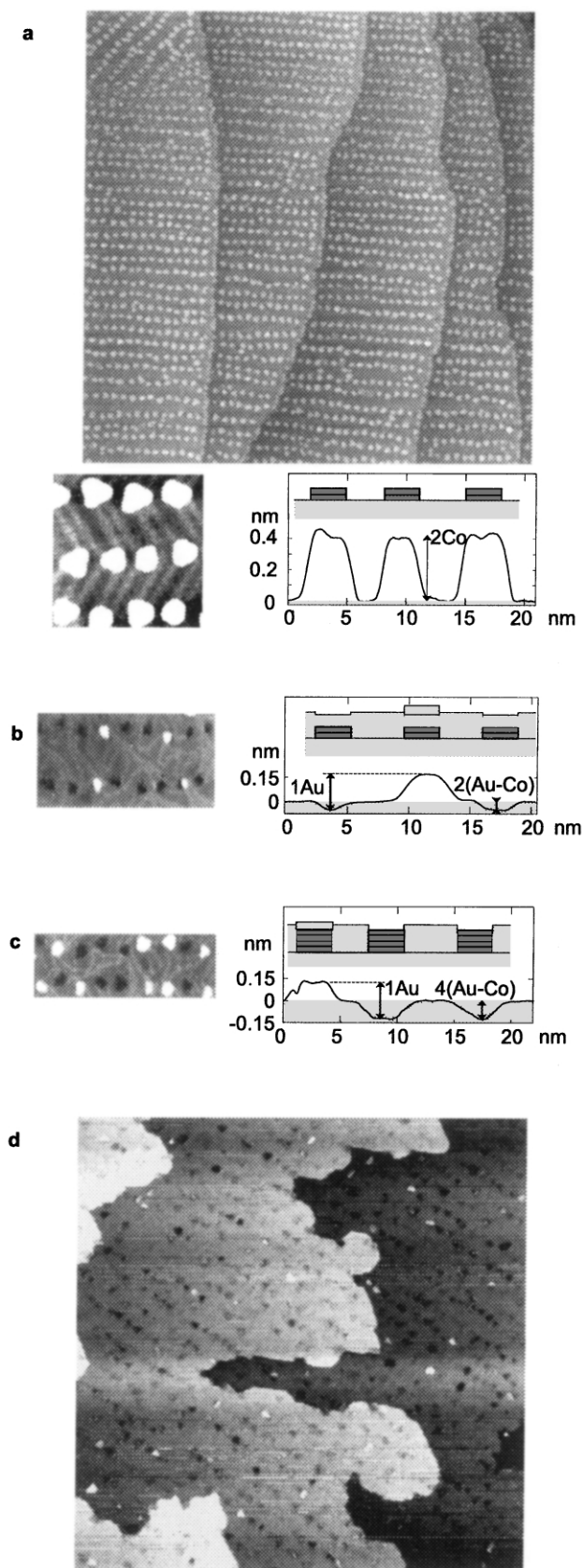


FIG. 1. Principle of multilayered systems of self-organized dots. (a) Strain energy minimization induces vertical self-alignment of dots from successive layers [4]. (b) Present process: dots come in vertical vicinity or even direct contact if the interlayer-spacer thickness is sufficiently reduced.



We now describe the deposition process. As a first step, 0.2 AL of Co is deposited on Au(111) at 300 K. As already known [1], 2 AL-high Co dots nucleate at the periodic kinks of the large-scale $22 \times \sqrt{3}$ Au reconstruction [6] (see Fig. 2a), resulting in self-organized parallel rows of dots. The rows are separated by approximately 13 nm, and the dot periodicity along a row is 7.5 nm. In this example, the dot diameter is 3 nm.

As a second step, the Co dots are covered with the amount of Au necessary to fill the space between the dots, and to complete up to the fourth Au atomic layer above the substrate. The temperature is raised from 425 to 475 K during deposition [7]. As Co atomic layers are slightly thinner than Au atomic layers, the buried array appears now as an array of hollows (Fig. 2b). This had already been noticed by other authors [8].

As a third step, 0.2 AL of Co is deposited at 500 K. This is the amount of Co that would be needed to increase the height of the previous Co dots by 2 AL, provided that the newly deposited Co atoms go on top of the buried dots. This is indeed what happens, as can be inferred from STM images (Fig. 2c). The array now displays both hollows and islands. Cross-section views of the STM images reveal that the hollows are ~ 0.12 nm deep, i.e., 4 times the height difference between a Au and a Co atomic layer. This suggests that a double-layer place-exchange mechanism took place between incoming Co atoms and Au atoms covering the buried Co dots from the previous layer. This mechanism is different from that occurring in step 1. Indeed, a close examination of Fig. 2b reveals that the kinks of the Au reconstructions are often displaced away from the dots after the Au deposition (step 2), and are no more regularly spaced. It can therefore be ruled out that the growth during step 3 (i.e., Co nucleation above the previous dots) is governed by the partial dislocation kinks. The place-exchange mechanism must rather be driven by surface energy and parameter misfit effects [9], which favor Co clustering. As for the islands, they are about 0.23 nm higher than the hollows, suggesting a decoration

FIG. 2. The pillar-growth process illustrated by STM views of the top surface. For steps (a)–(c), a cross-section view of real data is provided, along with a schematic view. (a) After deposition of a nominal thickness of 0.2 AL of Co on Au(111) at 300 K. The main STM image is 300×300 nm. The cross section reveals that the dots are 2 AL high. (b) After deposition of Au up to the completion of the fourth atomic layer (step 2 in the text). The STM image is 60×35 nm. The hollows are about 0.06 nm deep, which is consistent with twice the height difference between a bulk hcp Co(0001) AL (0.205 nm) and an fcc Au(111) AL (0.235 nm). (c) After deposition of the second layer of Co dots (step 3 in the text). The STM image is 65×25 nm. The hollows are about 0.12 nm deep, i.e., 4 times the height difference between a Co and a Au atomic layer, suggesting that the dots are now 4 AL high. (d) After 20 AL of Co have been stacked (300×300 nm STM image). A self-organized array of pillars of nearly pure Co has been formed, with pillars 3 nm in diameter and 5.5 nm high.

effect of some hollows by Au atoms expelled during the place-exchange mechanism. We add finally that no Co atoms were found at step edges either. This point is of great importance for the process, as the organization would be largely disturbed if new lines of randomly aggregated Co dots were nucleated at each step of the process.

As a fourth step, the amount of Au required to complete a smooth fifth layer is deposited at 500 K. The situation is then similar to that after step 2, but with 0.12 nm deep hollows. Starting from this point and maintaining the temperature at 500 K, we repeated many times a sequence where Co and Au are deposited alternately with nominal thicknesses of 0.1 and 0.9 AL, respectively. Repeating the type of observations discussed above, we deduced after each sequence that the newly deposited Co atoms aggregate on top of the previous Co dots, via a single-layer place-exchange mechanism with Au atoms. The organization is mainly undisturbed after 16 cycles (Fig. 2d). From this we believe to have fabricated continuous pillars of nearly pure Co on Au(111), with a vertical aspect ratio (height over diameter) of about 2:1.

We show in the following that the continuity of the pillars is confirmed by magnetic measurements. Two samples are examined. Sample *A* is the one depicted in Fig. 2. The pillars are ~ 3 nm in diameter and 5.5 nm high. Sample *B* contains pillars ~ 4.2 nm in diameter and 8 nm high. The volume of each pillar, as well as the estimated interpillar dipolar interactions, are expected to be about 3 times larger for sample *B* than for sample *A*. Besides, as both samples exhibit perpendicular magnetization, each pillar can be viewed as an Ising macrospin, either pointing up or down [10].

Sample *A* is superparamagnetic down to $T_B = 90$ K. The (reversible) perpendicular magnetization loops were analyzed using the $S = 1/2$ Brillouin function [11]. Dipolar fields coming from neighboring pillars were taken into account as an effective field, whose value was calculated self-consistently in a mean-field framework. Finally, we used to first approximation the Co bulk magnetization value. From this analysis of the data, we conclude that each independent magnetic entity holds an average of 2800 Co atoms, and that the interentity dipolar fields are demagnetizing and have a magnitude of 40 mT. These figures are in good agreement with those, calculated from the geometry of the pillars as determined by STM: 3300 Co atoms per pillar and 32 mT interpillar demagnetizing dipolar fields. This confirms that each pillar behaves as a single magnetic entity. Finally, the analysis of the remanent magnetization in sample *B* shows that $T_B \sim 300$ K (Fig. 3). The rise of T_B in sample *B* as compared to sample *A* ($T_B \sim 90$ K), and to the conventional flat Co dots ($T_B \sim 20$ K [12]), is ascribed to the increased pillar volume [3]. Note that none of the hysteretic curves were found to be dependent on the sweeping velocity of the magnetic field (in the

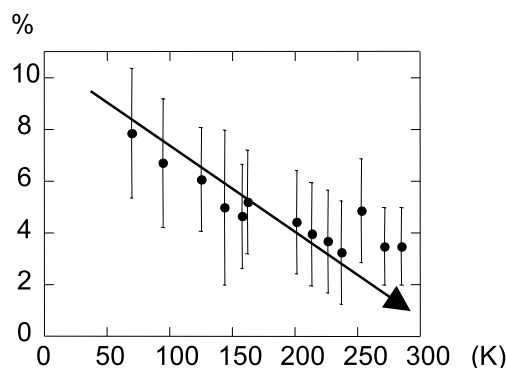


FIG. 3. Remanence versus temperature for Co pillars 4.2 nm in diameter and 8 nm high. The remanence was normalized by the saturation magnetization, so that $M_r = 1$ means full remanence. The vanishing of remanence defines the blocking temperature, $T_B \sim 300$ K [3]. In this sample the remanence remains smaller than 1 even at low temperature, because inter-pillar dipolar coupling within a chain favors antiferromagnetic alignment between neighbors.

range 0.01 to 0.5 T s $^{-1}$. Besides, we checked that the time constants of the measuring devices that we used did induce no artificial hysteresis on the magnetization curves.

As the Co/Au samples exhibit promising magnetic properties, it is interesting to discuss the versatility of the pillar growth process, in view of applying it to other materials. As Co and Au are immiscible in the bulk, the place-exchange mechanism must be driven by Au/Co parameter misfit and surface energy difference. This suggests that pillar growth should occur for other pairs of elements as well, with suitable parameter misfit and/or surface energy difference. Reports of Co self-burrowing on Au, Cu and Ag support this idea [13–15]. Besides, the process does not require self-organization to occur in the first layer; self-assembly is sufficient. This implies nearly no restriction on the materials, as self-assembly nearly always occurs in the submonolayer range of epitaxial growth, at least in a suitable temperature range. Moreover, the geometry of the pillars can, in principle, be fully tailored: the lateral density of pillars is determined by the island density in the submonolayer nucleation stage (play on temperature or deposition technique, like pulsed-laser deposition or molecular-beam epitaxy [16]), the width of the pillars by the amount of material deposited during each step, and their height by the number of stacked layers. These remarks open the way to the exciting concept of 3D self-engineering: in favorable cases, one might be able to design 3D nanostructures by stacking self-assembled and self-organized 2D structures step by step, in a way similar to the layer-by-layer tailoring of multilayered structures, designed to display specific properties.

Finally, the dramatic rise of blocking temperature achievable through pillar growth raises hope that high-density self-assembled media could one day be used in

commercial devices. Let us briefly discuss potential applications. Even when the pillars are called self-organized, as is the case of Co on Au(111), the lateral range of the order is at most some hundreds of nanometers. Naturally self-organized samples are therefore unsuitable for applications requiring a long-range order, such as recording media with one bit per pillar. With this respect, however, a promising technology for the future is the combination of lithography or nanoimprint to pattern a nucleation array, followed by self-assembly [17,18]. This would allow one to fabricate regular arrays of nearly monodisperse pillars with high-quality interfaces, and a high vertical aspect ratio. In the nearest future, the pillar growth process may find applications when the film as a whole (pillars plus matrix) is considered as a new artificial material with specific properties. Such a material might be used as a substitute for granular materials displaying giant magnetoresistance (GMR). The GMR magnitude may be enhanced as more independent parameters are available, and even more interestingly for devices, one could tune the interpillar dipolar coupling to decrease the saturation field, which in granular materials is too high for most devices [19].

In conclusion, we demonstrated that it is possible to grow nanometer-sized vertical pillars of one element into the surface of another element. The growth process is based on alternative depositions of each element, which allow one to replicate vertically the flat island pattern from the submonolayer range. We demonstrated the process with Co/Au, but it should also occur for other combinations, provided that the two elements show a significant difference of lattice mismatch or surface energy, and are not too much miscible. The process is of particular interest for magnetic systems, as it allows the superparamagnetic blocking temperature to be raised considerably, while keeping the lateral density of the dots unchanged.

We are grateful to G. Kröder for his skilled technical support.

*Corresponding author.

Email address: fruch@labs.polycnrs-gre.fr

Present address: Laboratoire Louis Néel (CNRS), BP166, 38042 Grenoble Cedex, France.

- [1] B. Voigtländer, G. Meyer, and N.M. Amer, Phys. Rev. B **44**, 10 354 (1991).
- [2] H. Brune, M. Giovannini, K. Bromann, and K. Kern, Nature (London) **394**, 451 (1998).
- [3] *Superparamagnetism*: in zero applied field, a dot with high uniaxial anisotropy K can be in two states, either up or down. At $T = 0$ K, the magnetization is frozen, the dot is fully remanent. When thermal energy becomes too large (namely, $25 \text{ kT} > KV$, with V the particle's volume) the dot is superparamagnetic; i.e., the spin fluctuates between up and down, even though the particle remains ferromagnetic (i.e., all electronic spins within a pillar remain aligned with each other at any given time). The crossover between the two regimes occurs at the blocking temperature T_B , determined experimentally by the cancellation of remanence.
- [4] Q. Xie, A. Madhukar, P. Chen, and N. Kobayashi, Phys. Rev. Lett. **75**, 2542 (1995).
- [5] It has been shown since that a more complex stacking, such as fcc, can occur in the case of materials with anisotropic elastic constants. See, e.g., G. Springholz, V. Holy, M. Pinczolits, and E. Bauer, Science **282**, 734 (1998).
- [6] J. Barth, H. Brune, G. Ertl, and R. Behm, Phys. Rev. B **42**, 9307 (1990).
- [7] We checked that the dots are very little affected by the annealing at 375 K. This was already known from Ref. [13].
- [8] J. Wollschläger and N. Amer, Surf. Sci. **277**, 1 (1992).
- [9] $\gamma_{\text{Co}} \sim 2.6 \text{ J m}^{-2}$ and $\gamma_{\text{Au}} \sim 1.4 \text{ J m}^{-2}$, and the in-plane lattice parameter misfit is 14%.
- [10] All pillar dimensions are smaller than the exchange length $\pi\sqrt{2A/\mu_0 M_s^2} \sim 9 \text{ nm}$, so that no domain wall nor vortex can be stabilized inside a pillar. A nearly single-domain magnetization state is therefore expected. Besides, the dipolar fields inside a row of pillars are demagnetizing for perpendicular magnetization (note that the estimated dipolar fields *between* the rows are negligible). These fields favor antiparallel magnetization alignment of neighboring pillars.
- [11] The $S = 1/2$ Brillouin function (\tanh) is relevant to describe the mean magnetization of an isolated (hypothesis 1) Ising spin (hypothesis 2) as a function of external applied field and temperature. Hypothesis 2 is justified by the high perpendicular anisotropy of the pillars (not discussed in the present paper). Hypothesis 1 is fulfilled by taking into account interpillar dipolar interactions as a mean effective field.
- [12] H. Dürr, S. Dhesi, E. Dudzik, D. Knabben, G. van der Laan, J. Goedkoop, and F. Hillebrecht, Phys. Rev. B **59**, R701 (1999).
- [13] S. Padovani, F. Scheurer, and J. Bucher, Europhys. Lett. **45**, 327 (1999).
- [14] M.Ø. Pedersen, I.A. Bönicke, E. Lægsgaard, I. Stensgaard, A. Ruban, J.K. Nørskov, and F. Besenbacher, Surf. Sci. **387**, 86 (1997).
- [15] C.G. Zimmermann, M. Yeadon, K. Nordlund, J.M. Gibson, R.S. Averback, U. Herr, and K. Samwer, Phys. Rev. Lett. **83**, 1163 (1999).
- [16] P. Ohresser, J. Shen, J. Barthel, M. Zheng, C. Mohan, M. Klaua, and J. Kirschner, Phys. Rev. B **59**, 3696 (1999).
- [17] T. Kamins, D. Ohlberg, R.S. Williams, W. Zhang, and S. Chou, Appl. Phys. Lett. **74**, 1773 (1999).
- [18] Y. Homma, P. Finnie, and T. Ogino, Appl. Phys. Lett. **74**, 815 (1999).
- [19] J. Daughton, J. Magn. Magn. Mater. **192**, 334 (1999).